spite their severely impaired growth, remained green and metabolically active for months, long after the WT died (*32*). These observations, in conjunction with the severe cytogenetic anomalies borne by late-generation mutants, imply that aspects of the primary cellular response to telomere dysfunction are unique to plants and may reflect the unusual plasticity of their development and genome organization. Nevertheless, an efficient telomere maintenance mechanism is crucial for indefinite cell proliferation and hence, telomerase-deficient *Arabidopsis* may offer new insight into pathways coordinating DNA checkpoint mechanisms and DNA repair.

**References and Notes**


1. V. Lundblad, *Proc. Natl. Acad. Sci. U.S.A.* **95**, 8415 (1998).
2. P. M. Lansdorp, *Mech. Ageing Dev.* **118**, 23 (2000).
3. R. Oulton, L. Harrington, *Curr. Opin. Oncol.* **12**, 74 (2000).
4. V. Lundblad, *Mutat. Res.* **451**, 227 (2000).
5. M. A. Blasco *et al.*, *Cell* **91**, 25 (1997).
6. H.-W. Lee *et al. Nature* **392**, 569 (1998).
7. L. Rudolph *et al. Cell* **96**, 729 (1999).
8. E. Herrera, E. Samper, M. A. Blasco, *EMBO J.* **18**, 1172 (1999).
9. L. Chin *et al. Cell* **97**, 527 (1999).
10. V. Walbot, *Trends Plant Sci.* **1**, 27 (1996).
11. $G_1$ mutants were obtained by selfing plants heterozygous for a T-DNA insertion in *AtTERT* (*12*). Five homozygous lines were generated from the progeny of individual $G_1$ plants, one from the WT (line 71) and four from mutant $G_1$ plants (lines 16, 20, 69, and 96). Individual lines were propagated through successive generations by selfing. Seeds from several plants within a single line were pooled in each generation until $G_6$. From $G_6$ onward, individual plants were examined. Plants were grown in continuous light at 21°C in an environmental growth chamber.
12. M. S. Fitzgerald *et al.*, *Proc. Natl. Acad. Sci. U.S.A.* **96**, 14813 (1999).
13. K. Riha, D. E. Shippen, unpublished data.
14. A. Kass-Eisler, C. W. Greider, *Trends Biochem. Sci.* **25**, 200 (2000).
15. M. P. Hande, E. Samper, P. Lansdorp, M. A. Blasco, *J. Cell Biol.* **144**, 589 (1999).
16. S. E. Artandi *et al.*, *Nature* **406**, 641 (2000).
17. K. E. Kirk, B. P. Harmon, I. K. Reichardt, J. W. Sedat, E. H. Blackburn, *Science* **275**, 1478 (1997).
18. Telomeres range in size from 2 to 4.5 kb in WT cells. In $G_6$ mutants, the longest telomeres were 2 kb; the shortest were only a few hundred base pairs (*13*).
19. The proportion of cells in mitosis [mitotic index (MI)] and the anaphase/metaphase ratio (A/M) were calculated for pistils from WT and class II/terminal plants. $MI_{WT} = 1.94 \pm 0.32$ ($n = 6$), $MI_{mutant} = 2.4 \pm 0.33$ ($n = 7$), $A/M_{WT} = 0.85 \pm 0.10$ ($n = 4$), $A/M_{mutant} = 0.83 \pm 0.06$ ($n = 5$).
20. Supplementary data are available on *Science* Online at www.sciencemag.org/cgi/content/full/291/5509/1797/DC1.
21. S. E. Clark, J. W. Schiefelbein, *Trends Cell Biol.* **7**, 454 (1997).
22. P. Laufs, O. Grandjean, C. Jonak, K. Kieu, J. Traas, *Plant Cell* **10**, 1375 (1998).
23. J. C. Fletcher, E. M. Meyerowitz, *Curr. Opin. Plant Biol.* **3**, 23 (2000).
24. E. M. Meyerowitz, *Cell* **88**, 299 (1997).
25. T. Laux, K. F. Mayer, *Semin. Cell Dev. Biol.* **9**, 195 (1998).
26. T. de Lange, T. Jacks, *Cell* **98**, 273 (1999).
27. J. Karlseder, D. Broccoli, Y. Dai, S. Hardy, T. de Lange, *Science* **283**, 1321 (1999).
28. K. Ahmad, K. G. Golic, *Genetics* **151**, 1041 (1999).
29. S. J. Klosterman, J. J. Choi, L. A. Hadwiger, *Physiol. Mol. Plant Pathol.* **56**, 197 (2000).
30. To investigate whether leaf cells respond to telomere depletion by apoptosis, we extracted genomic DNA from leaves of WT, $G_8$, and $G_9$ mutants using a DNeasy plant kit (Qiagen). DNA from four WT and six terminal plants was subjected to electrophoresis in a 1.5% agarose gel, transferred onto a Nylon membrane (MSI, Westborough, MA), and hybridized with radioactively labeled total genomic DNA. No difference in the DNA profiles was observed.
31. A. B. Bleecker, *Curr. Opin. Plant Biol.* **1**, 73 (1998).
32. WT plants grown at short day (8 hours of light) produced seeds after 10 weeks. Seed production was accompanied by senescence, and death occurred by the fourth month. In contrast, class II and some terminal mutants remained in the vegetative stage much longer and started to flower after 6 months.
33. J. S. Heslop-Harrison, in Arabidopsis *Protocols*, J. Martinez-Zapater, J. Salinas, Eds. (Humana, Totowa, NJ, 1998), vol. 82, p. 119.
34. J. Hughes, M. E. McCully, *Stain Technol.* **50**, 319 (1975).
35. V. Vasil, I. K. Vasil, in *Cell Culture and Somatic Cell Genetics of Plants* (Academic Press, London, 1984), vol. 1, p. 738.
36. Anthers were fixed in ethanol:acetic acid solution (3:1) and gently squashed in a drop of 60% acetic acid with a cover slip. Slides were observed by light microscopy.


37. We thank J. Chen, A. Pepper, P. Lansdorp, C. Price, and B. Vyskot for insightful comments on the manuscript. Funded by NSF grant MCB9982499 (T.D.M. and D.E.S) and a NATO-NSF postdoctoral fellowship (K.R.).

2 November 2000; accepted 22 January 2001


# Role of the Sphingosine-1-Phosphate Receptor EDG-1 in PDGF-Induced Cell Motility


**John P. Hobson,[1]* Hans M. Rosenfeldt,[1]* Larry S. Barak,[2] Ana Olivera,[1] Samantha Poulton,[1] Marc G. Caron,[2] Sheldon Milstien,[3] Sarah Spiegel[1]†**



**EDG-1 is a heterotrimeric guanine nucleotide binding protein–coupled receptor (GPCR) for sphingosine-1-phosphate (SPP). Cell migration toward platelet-derived growth factor (PDGF), which stimulates sphingosine kinase and increases intracellular SPP, was dependent on expression of EDG-1. Deletion of *edg-1* or inhibition of sphingosine kinase suppressed chemotaxis toward PDGF and also activation of the small guanosine triphosphatase Rac, which is essential for protrusion of lamellipodia and forward movement. Moreover, PDGF activated EDG-1, as measured by translocation of β-arrestin and phosphorylation of EDG-1. Our results reveal a role for receptor cross-communication in which activation of a GPCR by a receptor tyrosine kinase is critical for cell motility.**


Interest in SPP has accelerated recently with the discovery that it is the extracellular ligand for EDG-1, EDG-3, EDG-5, EDG-6, and EDG-8 (*1*). Although the biological functions of these GPCRs have not been completely elucidated, EDG-1 is implicated in cell migration, angiogenesis, and vascular maturation (*2–4*). Disruption of the *edg-1* gene by homologous recombination in mice resulted in massive intra-embryonic hemorrhaging and intrauterine death caused by incomplete vascular maturation resulting from a failure of mural cells—vascular smooth muscle cells and pericytes—to migrate to arteries and capillaries and to reinforce them properly (*4*). Disruption of the *PDGF-BB* or *PDGFR*-β genes in mice resulted in a similar lethal phenotype (*5*, *6*). Because in many different cell types, PDGF stimulates sphingosine kinase, leading to an accumulation of intracellular SPP (*1*, *7*), we speculated that interplay between PDGF and SPP–EDG-1 signals might be required for cell migratory responses. In this study, we found that activation of EDG-1 by the PDGFR plays a crucial role in regulating cell motility. The results reveal a new paradigm for communication between tyrosine kinase receptors and GPCRs.

Human embryonic kidney (HEK) 293 cells, which only express EDG-3 and EDG-5, did not migrate toward SPP unless EDG-1 was expressed (*2*). EDG-1 overexpression also stimulated migration of HEK 293 cells toward PDGF-BB (Fig. 1A), whereas migratory responses to serum and fibronectin were unaffected (Fig. 1A). Conversely, migration of mouse embryonic fibroblasts (MEFs), which express transcripts for EDG-1, EDG-3, and EDG-5, but not EDG-6 or EDG-8 (*4*), toward PDGF-BB was reduced when *edg-1* was deleted (Fig. 1B).


[1]Department of Biochemistry and Molecular Biology, Georgetown University Medical Center, Washington, DC 20007, USA. [2]Howard Hughes Medical Institute Laboratories and Department of Cell Biology, Duke University Medical Center, Durham, NC 27710, USA. [3]Laboratory of Cellular and Molecular Regulation, National Institute of Mental Health, Bethesda, MD 20892, USA

*These authors contributed equally to this report.
†To whom correspondence should be addressed. E-mail: spiegel@bc.georgetown.edu

A smaller effect on migration toward serum was observed in these mutant fibroblasts, and migration toward fibronectin was unaffected (Fig. 1B), indicating that *edg-1* deletion does not disrupt all essential mechanisms of directed cell movement.

Because the migration of smooth muscle cells appears to be aberrant in EDG-1 knockout mice (*4*), we also examined the role of EDG-1 in PDGF-directed migration of human aortic smooth muscle cells (ASMCs). Reduction of EDG-1 expression in ASMCs (which endogenously express EDG-1, EDG-3, and EDG-5) by EDG-1 antisense phosphothioate oligonucleotide (*3*), not only eliminated migration toward SPP but also reduced migration toward PDGF, but not serum (Fig. 1C). These results suggest that the loss of EDG-1 results in motility defects toward PDGF in diverse cell types. Dysfunctional migration of EDG-$1^{-/-}$ cells toward PDGF links this phenotype (*4*) to the *PDGF-BB* and *PDGFR*-β knockout phenotypes (*5*, *6*) at the final steps of vasculogenesis (*4*), underscoring the importance of cross-communication between PDGFR and EDG-1 in vascular maturation.

As it does in many other cell types (*1*, *7*), PDGF-BB stimulated sphingosine kinase activity in wild-type MEFs and had an even greater stimulatory effect in fibroblasts in which *edg-1* was deleted (Fig. 2A). To investigate whether SPP generated in response to PDGF might be involved in PDGF-mediated chemotaxis, we used *N*,*N*-dimethylsphingosine (DMS), a competitive inhibitor of sphingosine kinase (*8*). DMS inhibited PDGF-directed chemotaxis of wild-type MEFs (Fig. 2B) but did not reduce PDGF-stimulated receptor tyrosine phosphorylation (Fig. 2C). In agreement with its inability to interfere with binding of SPP to EDG-1 and its activation (*9*), DMS did not significantly affect chemotaxis of cells toward a gradient of SPP. Similarly, DMS also blocked formation of SPP and inhibited PDGF-directed chemotaxis of HEK 293 cells overexpressing EDG-1 (Fig. 2D). As these results indicate potential cross-talk between PDGF and EDG-1 signaling, and EDG-1 is mainly coupled to $G_i$ (*9*), cells were pretreated with pertussis toxin to inactivate $G_i$, which suppressed PDGF-induced chemotaxis

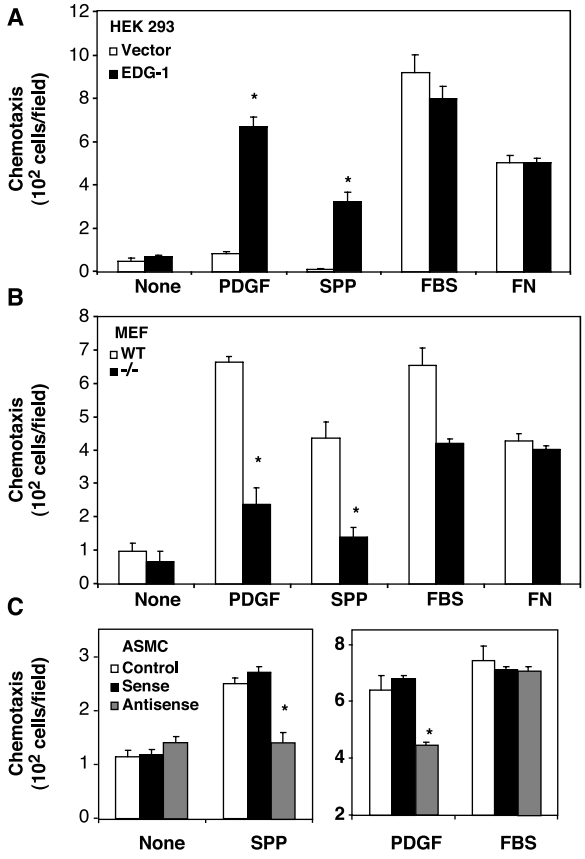


**Fig. 1.** Requirement of EDG-1 for PDGF-induced migration. (**A**) Enhanced chemotaxis toward PDGF in cells overexpressing EDG-1. HEK 293 cells stably transfected with vector (white bars) or EDG-1 (filled bars) were allowed to migrate toward PDGF-BB (20 ng/ml), SPP (100 nM), fetal bovine serum (FBS, 20%), or fibronectin (FN, 10 μg/ml). Chemotaxis was measured in a modified Boyden chamber assay (*2*). The average number of cells in four random fields was determined and is presented as the average ± SD of three individual wells. Similar results were obtained in at least three independent experiments, and statistically different groups are indicated by asterisk ($P < 0.05$ by analysis of variance). (**B**) Chemotaxis toward PDGF is markedly reduced by *edg-1* disruption. Wild-type (white bars) and EDG-$1^{-/-}$ (filled bars) MEFs were allowed to migrate toward PDGF-BB, SPP, serum, or FN as in (A). (**C**) Dependence of chemotaxis of ASMCs toward PDGF and SPP on EDG-1 expression. Human ASMCs were transfected without (white bars) or with 400 nM phosphothioate oligonucleotides [EDG-1 sense (filled bars), 5′-ATG GGG CCC ACC AGC GTC-3′; EDG-1 antisense (gray bars), 5′-GAC GCT GGT GGG CCC CAT-3′] using Lipofectamine (Life Technologies, Gaithersburg, Maryland) (*3*) and after 24 hours, were allowed to migrate toward SPP (100 nM), PDGF (20 ng/ml), or FBS (20%). Analysis by reverse transcriptase–polymerase chain reaction showed that EDG-1 mRNA expression was almost completely eliminated without affecting EDG-3 and EDG-5 expression.

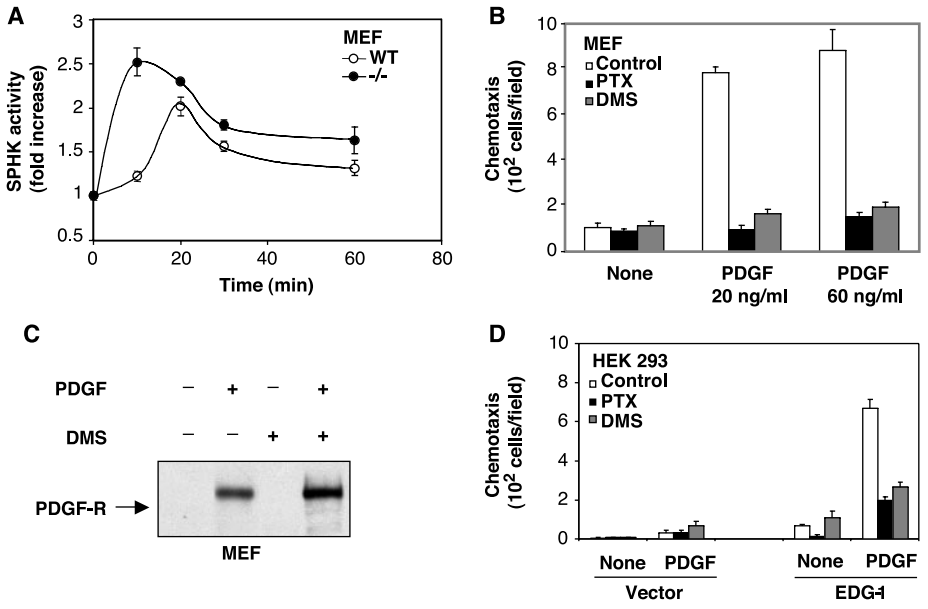


**Fig. 2.** Requirement of sphingosine kinase for PDGF-induced motility. (**A**) Stimulation of sphingosine kinase by PDGF in wild-type and EDG-$1^{-/-}$ MEFs. Wild-type and EDG-$1^{-/-}$ MEFs were treated with PDGF-BB (20 ng/ml) for the indicated times, and sphingosine kinase activity was measured. Basal activity was 114 ± 5 and 133 ± 2 pmol/min per milligram for wild-type and EDG-$1^{-/-}$ fibroblasts, respectively. (**B** and **D**) Inhibition of chemotaxis toward PDGF by the sphingosine kinase inhibitor DMS or pertussis toxin. Wild-type MEFs (B) or HEK 293 cells transfected with vector or EDG-1 (D) were treated without (control) or with pertussis toxin (PTX, 200 ng/ml, 2 hours), or DMS (10 μM, 20 min), then allowed to migrate toward the indicated concentrations of PDGF-BB, and chemotaxis was measured. (**C**) Lack of effect of DMS on tyrosine phosphorylation induced by PDGF. Wild-type MEFs were serum-starved for 24 hours, and then treated without or with DMS (10 μM) for 20 min, before stimulation with PDGF-BB (60 ng/ml) for 5 min. Equal amounts of cell-lysate proteins were analyzed by Western blotting using antibody against phosphotyrosine.

of both wild-type MEFs (Fig. 2B) and HEK 293 cells overexpressing EDG-1 (Fig. 2D).

Thus, EDG-1 appears to be necessary for PDGF-mediated chemotaxis. Therefore, we determined whether PDGF signaling might activate EDG-1 by regulating sphingosine kinase activity and accumulation of SPP, which in turn activates EDG-1. β-Arrestins are cytosolic proteins that bind with high affinity to agonist-activated, phosphorylated GPCRs to terminate receptor to G protein coupling. They also mediate receptor endocytosis (*10*, *11*) and initiation of a second wave of signaling (*12*, *13*). SPP promoted rapid redistribution of β-arrestin2 tagged with green fluorescent protein (GFP) from the cytoplasm to the plasma membrane only in EDG-1–expressing HEK 293 cells (Fig. 3A, part b). Treatment of cells overexpressing both EDG-1 and sphingosine kinase type 1 (SPHK1) with PDGF and sphingosine increased intracellular SPP and induced translocation of β-arrestin2 to the plasma membrane (Fig. 3B, part c), as did exposure of cells to exogenous SPP (Fig. 3B, part b). Availability of sphingosine is a limiting factor that influences levels of cellularly generated SPP (*14*). Thus, sphingosine-induced translocation of β-arrestin was dependent on overexpression of SPHK1 (note the lack of translocation in Fig. 3A, part c). Treatment with PDGF or sphingosine alone, or transfection with SPHK1 stimulated production of SPP by 2-, 6-, and 10-fold, respectively (Fig. 3C), but these concentrations of SPP did not result in significant translocation of β-arrestin. Treatment of SPHK1-expressing HEK 293 cells with a high concentration of sphingosine (Fig. 3B, part d) or sphingosine together with PDGF (Fig. 3B, part c), which increased SPP levels by 60- and 30-fold, respectively, resulted in translocation of β-arrestin to activated EDG-1. To determine the effect of PDGF alone, we used a more sensitive assay of GPCR activation because of the observation that activated GPCRs become phosphorylated before β-arrestin binding (*10*, *12*). To enhance sensitivity of detection, HEK 293 cells were cotransfected with expression plasmids encoding Flag epitope–tagged EDG-1 and PDGFR-β, labeled in situ with intracellular phosphate-32, and EDG-1 was immunoprecipitated with antibody against Flag. As did SPP (*15*), PDGF increased phosphorylation of EDG-1 in these cells (Fig. 3D), whereas no phosphorylation could be detected in vector-transfected cells (*16*).

Although these results suggest that endogenously generated SPP can activate EDG-1 and consequent translocation of β-arrestin, no significant release of SPP into the extracellular medium could be detected by mass measurements (<0.4 nM), even after treatment of SPHK1-expressing HEK 293 cells with PDGF-BB and sphingosine to increase SPP. To examine the possibility that amounts of SPP below our mass detection limits may in fact be secreted into the vicinity of EDG-1 and may activate

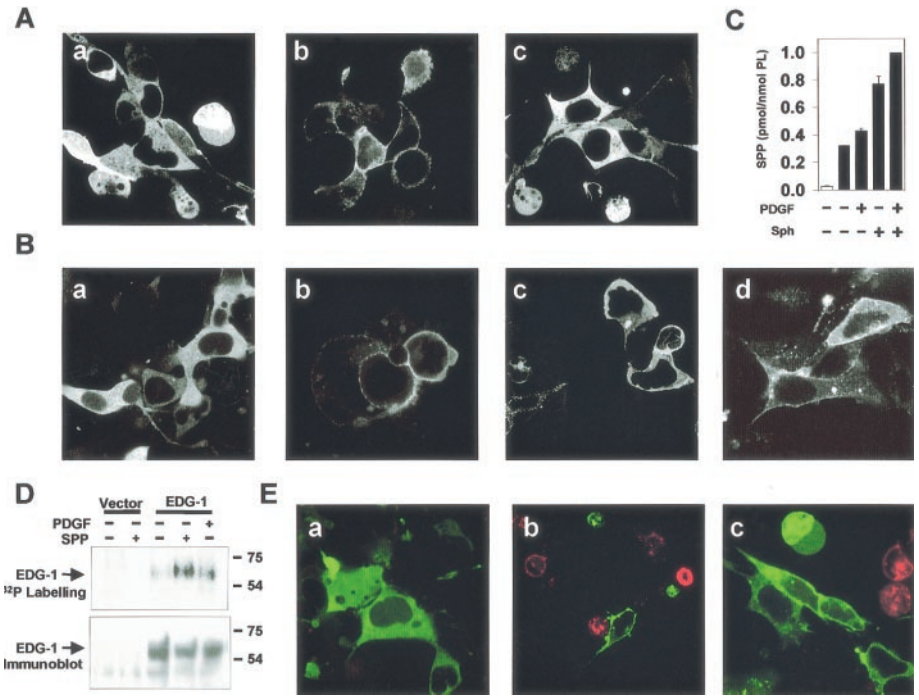


**Fig. 3.** SPP produced intracellularly can act in an autocrine or paracrine fashion to activate EDG-1. (**A**) β-Arrestin translocation in HEK 293 cells cotransfected with expression plasmids encoding β-arrestin2–GFP and EDG-1. β-Arrestin2–GFP fluorescence was visualized (*10*) after treatment with vehicle (a), 100 nM SPP (b), or 5 μM sphingosine (c). (**B**) Translocation of β-arrestin in HEK 293 cells cotransfected with β-arrestin2–GFP, EDG-1, and SPHK1. β-Arrestin2–GFP fluorescence was visualized after treatment with vehicle (a), 100 nM SPP (b), 2.5 μM sphingosine and 20 ng/ml PDGF-BB (c), or 5 μM sphingosine (d). (**C**) Cellular levels of SPP. Levels of SPP were measured in vector-transfected (white bar) and in SPHK1-transfected (filled bars) HEK 293 cells after treatment with 2.5 μM sphingosine, 20 ng/ml PDGF-BB, or both for 10 min (*20*). (**D**) PDGF-induced EDG-1 phosphorylation. Vector or Flag–EDG-1–expressing HEK 293 cells were transfected with PDGFR-β and cultured in 10% charcoal-stripped FBS for 24 hours, metabolically labeled in phosphate-free Dulbecco's modified Eagle's medium with [$^{32}$P]orthophosphate (70 μCi/ml) for 2.5 hours at 37°C, then stimulated with SPP (100 nM) or PDGF (20 ng/ml). Cell lysates were prepared and immunoprecipitated with antibody against Flag M2 (Sigma) as described (*15*). Immunoprecipitates were either separated on 10% SDS-PAGE, transblotted to nitrocellulose, and autoradiographed (upper panel) or immunoblotted with antibody against Flag (lower panel). (**E**) β-Arrestin translocation in HEK 293 cells cotransfected with β-arrestin2–GFP, EDG-1, and empty vector for SPHK1 (green cells). Conditioned medium from β-arrestin2–RFP, EDG-1, and SPHK1 transfectants (red cells) that had been treated with 5 μM sphingosine to generate intracellular SPP (a) or the cells themselves (b and c) were added to "green" cells. β-Arrestin2–GFP and β-arrestin2–RFP fluorescence was visualized by using dual excitation (488 and 568 nm) and emission (515 to 540 nm, GFP; 590 to 610 nm, RFP) filter sets (*10*).

it, SPHK1-expressing cells were transfected with β-arrestin2 fused to red fluorescent protein (RFP) at the $NH_2$-terminus (red) to differentiate them from β-arrestin2–GFP (green) transfectants. The β-arrestin2–RFP transfectants were treated with 5 μM sphingosine to increase intracellular SPP maximally. Conditioned medium from these SPP-producing cells did not induce translocation of β-arrestin2–GFP in EDG-1–transfected cells (Fig. 3E, part a). Nevertheless, coculturing of "red" SPP-producing cells with "green" EDG-1–transfected cells induced translocation of β-arrestin2–GFP to the plasma membrane on adjacent cells (Fig. 3E, part b) and on distant cells (Fig. 3E, part c). These results suggest that endogenously generated SPP can activate EDG-1 in an autocrine or paracrine manner.

Although deletion of *edg-1* or uncoupling $G_i$ inhibited PDGF-directed motility, there were no significant differences in PDGFR expression or PDGF-stimulated receptor tyrosine phosphorylation in wild-type compared with EDG-1 null fibroblasts (Fig. 4A). Rac, a member of the Rho family of small guanosine triphosphatases (Rac, Cdc42, and Rho), plays a critical role in cell motility by regulating formation of new lamellipodial protrusions at the leading edge (*17*). PDGF-BB rapidly activated Rac (Fig. 4B), but not Cdc42, in wild-type fibroblasts. Deletion of *edg-1* or inhibition of sphingosine kinase in wild-type MEFs decreased Rac activation induced by PDGF. These results suggest that Rac may participate in integration of PDGFR and EDG-1 signaling to promote cell migration and that the SPP signaling pathway may be important to amplify activation of Rac.

Various agonists for GPCRs can activate growth factor tyrosine kinase receptors in the absence of added growth factors (*18*). Al-

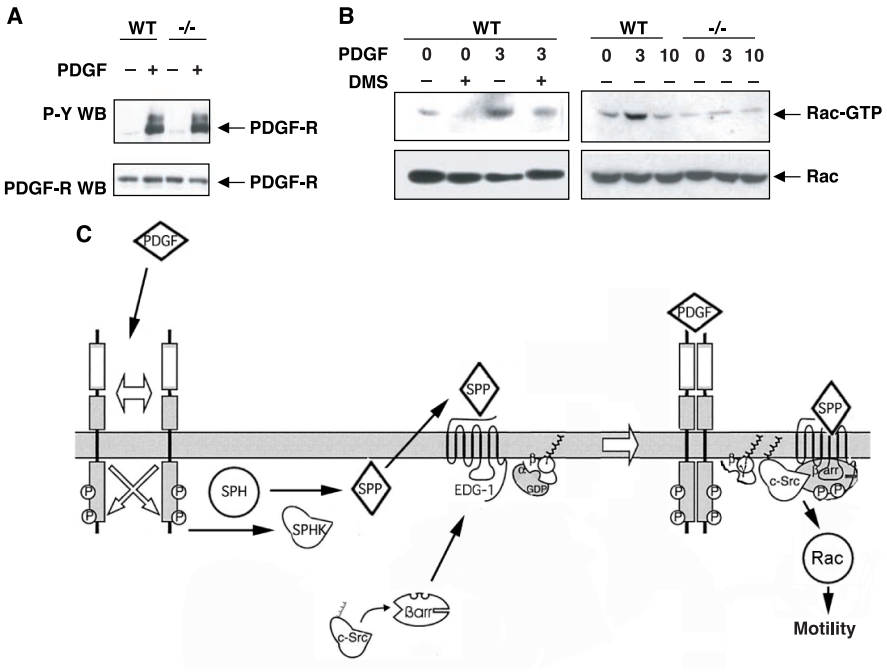


**Fig. 4.** Effect of *edg-1* deletion on PDGF signaling. (**A**) Deletion of *edg-1* has no effect on PDGF-induced tyrosine phosphorylation of PDGFR. Wild-type and EDG-1$^{-/-}$ MEFs were serum-starved for 24 hours, and then treated without or with PDGF-BB (20 ng/ml) for 5 min. Equal amounts of cell-lysate proteins were analyzed by Western blotting with antibody against phosphotyrosine. Blots were then stripped and reprobed with polyclonal antibody against PDGFR (Upstate Biotechnology, Lake Placid, New York). (**B**) Deletion of *edg-1* or inhibition of sphingosine kinase diminishes PDGF-mediated Rac activation. Wild-type and EDG-1$^{-/-}$ MEFs were treated with PDGF-BB (50 ng/ml) for the indicated times in the absence or presence of pretreatment with DMS (20 μM) for 20 min as indicated. Cell lysates were incubated with immobilized PAK-1 binding domain (Upstate Biotechnology) and associated GTP-Rac was determined by Western blotting using a specific Rac antibody or used without affinity immunoprecipitation to determine total Rac levels as shown below (*4*). (**C**) Activation of EDG-1 by PDGF. Scheme for intracellular communication between tyrosine kinase growth factor receptor (PDGFR) and GPCR (EDG-1) signaling pathways.

though this type of cross-communication is important for regulation of cell growth (*18*), our results suggest that cell motility is regulated by a reciprocal mechanism of receptor cross-talk. Thus, a tantalizing notion is that spatially and temporally localized generation of SPP by activation of sphingosine kinase in response to PDGF results in restricted activation of the GPCR EDG-1 that in turn activates Rac (Fig. 4C). Rac may then amplify the initial receptor signals (*19*), thus creating a positive feedback loop at the leading edge of the cell.


**References and Notes**

1. S. Spiegel, S. Milstien, *Biochim. Biophys. Acta* **1484**, 107 (2000).
2. F. Wang *et al.*, *J. Biol. Chem.* **274**, 35343 (1999).
3. M. J. Lee *et al.*, *Cell* **99**, 301 (1999).
4. Y. Liu *et al.*, *J. Clin. Invest.* **106**, 951 (2000).
5. P. Lindahl, B. R. Johansson, P. Leveen, C. Betsholtz, *Science* **277**, 242 (1997).
6. M. Hellstrom, M. Kaln, P. Lindahl, A. Abramsson, C. Betsholtz, *Development* **126**, 3047 (1999).
7. A. Olivera, S. Spiegel, *Nature* **365**, 557 (1993).
8. L. C. Edsall, J. R. Van Brocklyn, O. Cuvillier, B. Kleuser, S. Spiegel, *Biochemistry* **37**, 12892 (1998).
9. J. R. Van Brocklyn *et al.*, *J. Cell Biol.* **142**, 229 (1998).
10. R. H. Oakley, S. A. Laporte, J. A. Holt, L. S. Barak, M. G. Caron, *J. Biol. Chem.* **274**, 32248 (1999).
11. S. A. Laporte *et al.*, *Proc. Natl. Acad. Sci. U.S.A.* **96**, 3712 (1999).
12. L. M. Luttrell *et al.*, *Science* **283**, 655 (1999).
13. P. H. McDonald *et al.*, *Science* **290**, 1574 (2000).
14. A. Olivera *et al.*, *J. Cell Biol.* **147**, 545 (1999).
15. M. J. Lee, S. Thangada, C. H. Liu, B. D. Thompson, T. Hla, *J. Biol. Chem.* **273**, 22105 (1998).
16. PDGF also induced phosphorylation of EDG-1 in *myc*–EDG-1–transfected NIH 3T3 fibroblasts, which express high endogenous levels of PDGF-β and PDGF-α receptors.
17. A. Hall, *Science* **279**, 509 (1998).
18. N. Prenzel *et al.*, *Nature* **402**, 884 (1999).
19. G. Servant *et al.*, *Science* **287**, 1037 (2000).
20. L. C. Edsall, S. Spiegel, *Anal. Biochem.* **272**, 80 (1999).


21. Supported by NIH grant GM43880 to S.S. and in part by NIH grants CA61774 to S.S., HL-61365 to L.S.B., and NS19576 to M.G.C.; predoctoral fellowship from the U.S. Army Medical Research and Material Command to J.P.H.; and postdoctoral fellowship from the American Heart Association to H.M.R. We thank R. Proia and Y. Liu for generously providing us with MEFs and for helpful discussions.

12 December 2000; accepted 25 January 2001


# The Role of Working Memory in Visual Selective Attention


**Jan W. de Fockert,[1]* Geraint Rees,[2] Christopher D. Frith,[3] Nilli Lavie[1]**



**The hypothesis that working memory is crucial for reducing distraction by maintaining the prioritization of relevant information was tested in neuroimaging and psychological experiments with humans. Participants performed a selective attention task that required them to ignore distractor faces while holding in working memory a sequence of digits that were in the same order (low memory load) or a different order (high memory load) on every trial. Higher memory load, associated with increased prefrontal activity, resulted in greater interference effects on behavioral performance from the distractor faces, plus increased face-related activity in the visual cortex. These findings confirm a major role for working memory in the control of visual selective attention.**


Despite a vast body of research on visual attention and on working memory, the interaction between the two has seldom been addressed. There have been a few recent suggestions that working memory may play a role in the control of selective attention (*1*, *2*), but evidence for a specific role has been scarce. Here we show a direct causal role for working memory in the control of selective attention.

The most enduring issue in the study of attention is the extent to which distractor processing can be prevented (*3*). Lavie recently proposed that the level of perceptual load in a display is a crucial factor (*4*). Several studies have shown that distractors that could not be ignored in situations of low perceptual load (for example, when just a few task-relevant stimuli were presented) were successfully ignored in situations of high perceptual load (for example, when many relevant stimuli were present). Thus, less distrac-


[1]Department of Psychology, University College London, Gower Street, London WC1E 6BT, UK. [2]Institute of Cognitive Neuroscience, University College London, Alexandra House, 17 Queen Square, London WC1N 3AR, UK. [3]Wellcome Department of Cognitive Neurology, Institute of Neurology, 12 Queen Square, London WC1N 3BG, UK.

*To whom correspondence should be addressed. E-mail: j.de-fockert@ucl.ac.uk